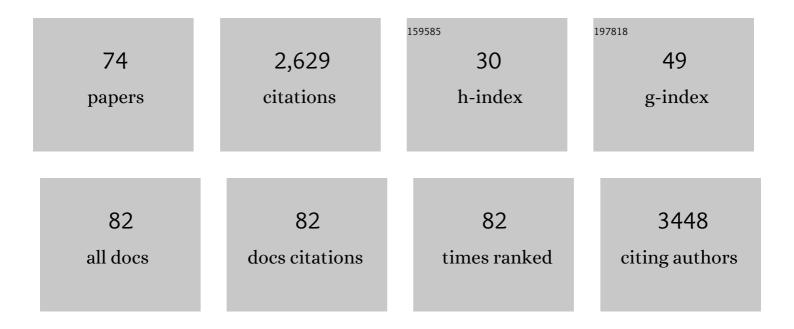
List of Publications by Year in descending order

Source: https://exaly.com/author-pdf/6241112/publications.pdf Version: 2024-02-01



CANC REN

| # | Article | IF | CITATIONS |
|----|------------------------------------------------------------------------------------------------------------------------------------------------------------------------------------------------------------|------|-----------|
| 1 | Designed and biologically active protein lattices. Nature Communications, 2021, 12, 3702. | 12.8 | 25 |
| 2 | Discovery of Stable and Selective Antibody Mimetics from Combinatorial Libraries of Polyvalent, Loop-Functionalized Peptoid Nanosheets. ACS Nano, 2020, 14, 185-195. | 14.6 | 38 |
| 3 | Real-time observation of dynamic structure of liquid-vapor interface at nanometer resolution in electron irradiated sodium chloride crystals. Scientific Reports, 2020, 10, 8596. | 3.3 | 6 |
| 4 | Extended harmonic mapping connects the equations in classical, statistical, fluid, quantum physics and general relativity. Scientific Reports, 2020, 10, 18281. | 3.3 | 0 |
| 5 | Allosteric regulation of lysosomal enzyme recognition by the cation-independent mannose 6-phosphate receptor. Communications Biology, 2020, 3, 498. | 4.4 | 20 |
| 6 | LoTToR: An Algorithm for Missing-Wedge Correction of the Low-Tilt Tomographic 3D Reconstruction of a Single-Molecule Structure. Scientific Reports, 2020, 10, 10489. | 3.3 | 26 |
| 7 | A DNA origami plasmonic sensor with environment-independent read-out. Nano Research, 2019, 12, 2900-2907. | 10.4 | 2 |
| 8 | Single-molecule 3D imaging of human plasma intermediate-density lipoproteins reveals a polyhedral structure. Biochimica Et Biophysica Acta - Molecular and Cell Biology of Lipids, 2019, 1864, 260-270. | 2.4 | 15 |
| 9 | Single-Molecule 3D Images of "Hole-Hole―lgG1 Homodimers by Individual-Particle Electron Tomography. Scientific Reports, 2019, 9, 8864. | 3.3 | 11 |
| 10 | Optimized Negative-Staining Protocol for Lipid–Protein Interactions Investigated by Electron Microscopy. Methods in Molecular Biology, 2019, 2003, 163-173. | 0.9 | 4 |
| 11 | Control of Amphiphile Self-Assembly via Bioinspired Metal Ion Coordination. Journal of the American Chemical Society, 2018, 140, 1409-1414. | 13.7 | 62 |
| 12 | Three-dimensional structural dynamics of DNA origami Bennett linkages using individual-particle electron tomography. Nature Communications, 2018, 9, 592. | 12.8 | 48 |
| 13 | Effect of curcumin on amyloidâ€like aggregates generated from methionineâ€oxidized apolipoprotein Aâ€l. FEBS Open Bio, 2018, 8, 302-310. | 2.3 | 9 |
| 14 | An Algorithm for Enhancing the Image Contrast of Electron Tomography. Scientific Reports, 2018, 8, 16711. | 3.3 | 9 |
| 15 | Structural Plasticity of Neurexin 1α: Implications for its Role as Synaptic Organizer. Journal of Molecular Biology, 2018, 430, 4325-4343. | 4.2 | 10 |
| 16 | IgG Antibody 3D Structures and Dynamics. Antibodies, 2018, 7, 18. | 2.5 | 39 |
| 17 | Structural basis of the lipid transfer mechanism of phospholipid transfer protein (PLTP). Biochimica Et Biophysica Acta - Molecular and Cell Biology of Lipids, 2018, 1863, 1082-1094. | 2.4 | 17 |
| 18 | A facile method for isolation of recombinant human apolipoprotein A-I from E.Âcoli. Protein Expression and Purification, 2017, 134, 18-24. | 1.3 | 4 |

| # | Article | IF | CITATIONS |
|----|---------------------------------------------------------------------------------------------------------------------------------------------------------------------------------------|------|-----------|
| 19 | Assessing the mechanisms of cholesteryl ester transfer protein inhibitors. Biochimica Et Biophysica Acta - Molecular and Cell Biology of Lipids, 2017, 1862, 1606-1617. | 2.4 | 15 |
| 20 | Extended theory of harmonic maps connects general relativity to chaos and quantum mechanism. Chaos, Solitons and Fractals, 2017, 103, 567-570. | 5.1 | 5 |
| 21 | Structural and Functional Characterization of a Hole–Hole Homodimer Variant in a "Knob-Into-Hole― Bispecific Antibody. Analytical Chemistry, 2017, 89, 13494-13501. | 6.5 | 31 |
| 22 | Fully Mechanically Controlled Automated Electron Microscopic Tomography. Scientific Reports, 2016, 6, 29231. | 3.3 | 19 |
| 23 | Polyhedral 3D structure of human plasma very low density lipoproteins by individual particle cryo-electron tomography1. Journal of Lipid Research, 2016, 57, 1879-1888. | 4.2 | 26 |
| 24 | Three Dimensional Dynamics and Fluctuations of DNA-Nanogold Dimers by Individual-Particle Electron Tomography. Biophysical Journal, 2016, 110, 184a. | 0.5 | 0 |
| 25 | Insights into the Tunnel Mechanism of Cholesteryl Ester Transfer Protein through All-atom Molecular Dynamics Simulations. Journal of Biological Chemistry, 2016, 291, 14034-14044. | 3.4 | 25 |
| 26 | Molecular Architecture of Contactin-associated Protein-like 2 (CNTNAP2) and Its Interaction with Contactin 2 (CNTN2). Journal of Biological Chemistry, 2016, 291, 24133-24147. | 3.4 | 47 |
| 27 | Three-dimensional structural dynamics and fluctuations of DNA-nanogold conjugates by individual-particle electron tomography. Nature Communications, 2016, 7, 11083. | 12.8 | 36 |
| 28 | Large Conformational Changes of Insertion 3 in Human Glycyl-tRNA Synthetase (hGlyRS) during Catalysis. Journal of Biological Chemistry, 2016, 291, 5740-5752. | 3.4 | 14 |
| 29 | Electron Tomography: A Threeâ€Dimensional Analytic Tool for Hard and Soft Materials Research. Advanced Materials, 2015, 27, 5638-5663. | 21.0 | 152 |
| 30 | HDL surface lipids mediate CETP binding as revealed by electron microscopy and molecular dynamics simulation. Scientific Reports, 2015, 5, 8741. | 3.3 | 48 |
| 31 | 3D Structural Fluctuation of IgG1 Antibody Revealed by Individual Particle Electron Tomography. Scientific Reports, 2015, 5, 9803. | 3.3 | 104 |
| 32 | Surface Density-Induced Pleating of a Lipid Monolayer Drives Nascent High-Density Lipoprotein Assembly. Structure, 2015, 23, 1214-1226. | 3.3 | 36 |
| 33 | Cationic lipid nanodisks as an siRNA delivery vehicle. Biochemistry and Cell Biology, 2014, 92, 200-205. | 2.0 | 31 |
| 34 | Calsyntenin-3 Molecular Architecture and Interaction with Neurexin 11±. Journal of Biological Chemistry, 2014, 289, 34530-34542. | 3.4 | 47 |
| 35 | Visualizing Biological Samples in Liquid Solution by Electron Microscopy. Biophysical Journal, 2014, 106, 598a. | 0.5 | 0 |
| 36 | Determination of the Dynamic Structures of Igg Antibody by Individual-Particle Electron Tomography. Biophysical Journal, 2014, 106, 251a. | 0.5 | 0 |

| # | Article | IF | CITATIONS |
|----|---------------------------------------------------------------------------------------------------------------------------------------------------------------------------------------------|-----|-----------|
| 37 | Optimized Negative Staining: a High-throughput Protocol for Examining Small and Asymmetric Protein Structure by Electron Microscopy. Journal of Visualized Experiments, 2014, , e51087. | 0.3 | 60 |
| 38 | Structure and Function of Cholesteryl Ester Transfer Protein in Cholesterol Transferring. Biophysical Journal, 2013, 104, 166a. | 0.5 | 0 |
| 39 | Structural features of cholesteryl ester transfer protein: A molecular dynamics simulation study. Proteins: Structure, Function and Bioinformatics, 2013, 81, 415-425. | 2.6 | 24 |
| 40 | A 3-D Image of an Individual Protein. Biophysical Journal, 2013, 104, 176a. | 0.5 | 0 |
| 41 | Optimized Negative-Staining Protocol for Examining Lipid-Protein Interactions by Electron Microscopy. Methods in Molecular Biology, 2013, 974, 111-118. | 0.9 | 5 |
| 42 | Optimized negative-staining electron microscopy for lipoprotein studies. Biochimica Et Biophysica Acta - General Subjects, 2013, 1830, 2150-2159. | 2.4 | 50 |
| 43 | Peptide-Conjugation Induced Conformational Changes in Human IgG1 Observed by Optimized Negative-Staining and Individual-Particle Electron Tomography. Scientific Reports, 2013, 3, 1089. | 3.3 | 30 |
| 44 | Asymmetric Small Protein Structure Determination by Individual Particle Electron Tomography. Biophysical Journal, 2012, 102, 394a. | 0.5 | 4 |
| 45 | Structural basis of transfer between lipoproteins by cholesteryl ester transfer protein. Nature Chemical Biology, 2012, 8, 342-349. | 8.0 | 123 |
| 46 | IPET and FETR: Experimental Approach for Studying Molecular Structure Dynamics by Cryo-Electron Tomography of a Single-Molecule Structure. PLoS ONE, 2012, 7, e30249. | 2.5 | 75 |
| 47 | High-Resolution Single-Molecule Structure Revealed by Electron Microscopy and Individual Particle Electron Tomography. , 2012, 02, . | | 4 |
| 48 | Title is missing!. Progress in Biochemistry and Biophysics, 2012, 39, 972-978. | 0.3 | 0 |
| 49 | Membraneâ€directed molecular assembly of the neuronal SNARE complex. Journal of Cellular and Molecular Medicine, 2011, 15, 31-37. | 3.6 | 29 |
| 50 | Morphology and structure of lipoproteins revealed by an optimized negative-staining protocol of electron microscopy. Journal of Lipid Research, 2011, 52, 175-184. | 4.2 | 101 |
| 51 | An optimized negative-staining protocol of electron microscopy for apoE4•POPC lipoprotein. Journal of Lipid Research, 2010, 51, 1228-1236. | 4.2 | 52 |
| 52 | Assessment of the Validity of the Double Superhelix Model for Reconstituted High Density Lipoproteins. Journal of Biological Chemistry, 2010, 285, 41161-41171. | 3.4 | 56 |
| 53 | Cholesteryl Ester Transfer Protein Penetrates Lipoproteins For Cholesteryl Ester Transfer. Biophysical Journal, 2010, 98, 36a. | 0.5 | 2 |
| 54 | Model of human low-density lipoprotein and bound receptor based on CryoEM. Proceedings of the National Academy of Sciences of the United States of America, 2010, 107, 1059-1064. | 7.1 | 65 |

| # | Article | IF | CITATIONS |
|----|-------------------------------------------------------------------------------------------------------------------------------------------------------------------------------------------------------------------------------------------------|-----|-----------|
| 55 | Structure of membraneâ€associated neuronal SNARE complex: implication in neurotransmitter release. Journal of Cellular and Molecular Medicine, 2009, 13, 4161-4165. | 3.6 | 27 |
| 56 | Apolipoprotein Al tertiary structures determine stability and phospholipidâ€binding activity of discoidal highâ€density lipoprotein particles of different sizes. Protein Science, 2009, 18, 921-935. | 7.6 | 30 |
| 57 | Nanoscale 3D contour map of protein assembly within the astrocyte porosome complex. Cell Biology International, 2009, 33, 224-229. | 3.0 | 13 |
| 58 | Nanodisks Derived from Amphotericin B Lipid Complex. Journal of Pharmaceutical Sciences, 2008, 97, 4425-4432. | 3.3 | 23 |
| 59 | EM 3D contour maps provide protein assembly at the nanoscale within the neuronal porosome complex. Journal of Microscopy, 2008, 232, 106-111. | 1.8 | 37 |
| 60 | Amphotericin B induces interdigitation of apolipoprotein stabilized nanodisk bilayers. Biochimica Et Biophysica Acta - Biomembranes, 2008, 1778, 303-312. | 2.6 | 20 |
| 61 | The Interplay between Size, Morphology, Stability, and Functionality of High-Density Lipoprotein Subclasses. Biochemistry, 2008, 47, 4770-4779. | 2.5 | 84 |
| 62 | Structure of apolipoprotein A-I in spherical high density lipoproteins of different sizes. Proceedings of the National Academy of Sciences of the United States of America, 2008, 105, 12176-12181. | 7.1 | 182 |
| 63 | The Architecture of a Water-Selective Pore in the Lipid Bilayer Visualized by Electron Crystallography in Vitreous Ice. Novartis Foundation Symposium, 2008, , 33-50. | 1.1 | 4 |
| 64 | Single-particle Image Reconstruction of a Tetramer of HIV Integrase Bound to DNA. Journal of Molecular Biology, 2007, 366, 286-294. | 4.2 | 41 |
| 65 | Neuronal fusion pore assembly requires membrane cholesterol. Cell Biology International, 2007, 31, 1301-1308. | 3.0 | 59 |
| 66 | Model of the toxic complex of anthrax: Responsive conformational changes in both the lethal factor and the protective antigen heptamer. Protein Science, 2006, 15, 2190-2200. | 7.6 | 22 |
| 67 | Large-Scale Structural Changes Accompany Binding of Lethal Factor to Anthrax Protective Antigen. Structure, 2004, 12, 2059-2066. | 3.3 | 25 |
| 68 | Supine Orientation of a Murine MHC Class I Molecule on the Membrane Bilayer. Current Biology, 2004, 14, 718-724. | 3.9 | 29 |
| 69 | Conversion of a Mechanosensitive Channel Protein from a Membrane-embedded to a Water-soluble Form by Covalent Modification with Amphiphiles. Journal of Molecular Biology, 2004, 343, 747-758. | 4.2 | 15 |
| 70 | Visualization of a water-selective pore by electron crystallography in vitreous ice. Proceedings of the National Academy of Sciences of the United States of America, 2001, 98, 1398-1403. | 7.1 | 79 |
| 71 | 3D reconstruction from electron micrographs of tilted 2D crystal: structure of a human water channel. , 2000, 4123, 224. | | 0 |
| 72 | Three-dimensional fold of the human AQP1 water channel determined at 4 Ã resolution by electron crystallography of two-dimensional crystals embedded in ice 1 1Edited by W. Baumeister. Journal of Molecular Biology, 2000, 301, 369-387. | 4.2 | 72 |

| # | Article | IF | CITATIONS |
|----|-------------------------------------------------------------------------------------------------------------------------------------------------------------------------|-----|-----------|
| 73 | Polymorphism in the Packing of Aquaporin-1 Tetramers in 2-D Crystals. Journal of Structural Biology, 2000, 130, 45-53. | 2.8 | 18 |
| 74 | Robust Parameterization of Elastic and Absorptive Electron Atomic Scattering Factors. Acta Crystallographica Section A: Foundations and Advances, 1996, 52, 257-276. | 0.3 | 170 |